BABEȘ-BOLYAI UNIVERSITY

FACULTY OF PHYSICS

DOCTORAL SCHOOL OF PHYSICS

SERS-based liquid biopsy for clinical applications

Summary of the PhD Thesis

PhD candidate:

Ramona-Gabriela COZAN

Scientific coordinator:

Prof. dr. Nicolae LEOPOLD

Cluj-Napoca

2026

Content

LIST OF PUBLICATIONS AND CONFERENCES

Publications on the subject of the thesis

1. S. D. Iancu, **R. G. Cozan**, O. M. Biro, V. Moisoiu and N. Leopold, "Label-free SERS liquid biopsy for medical diagnostics" in *Vibrational Biospectroscopy*, Bayden Wood & Max Diem Eds., Wiley (accepted).

2. D. Andras, **R. G. Cozan**, D. E. Muresan, V. Moisoiu, G. Crisan, V. Bintintan, G. C. Dindelegan, N. Leopold, and S. D. Iancu, "Advancing breast cancer diagnosis: Optimization of Raman spectroscopy for urine-based early detection", *Biomedicines*, vol. 13, no. 2, p. 505, 2025, doi: 10.3390/biomedicines13020505. (Q2, IF: 3.9, AIS: 0.89)

3. D. Andras, S. D. Iancu, **R. G. Cozan**, M. Zetes, G. Crisan, C. F. Buldus, I. Andras, V. Bintintan, G. C. Dindelegan, and N. Leopold, "SERS liquid biopsy in colorectal cancer detection and treatment response: Revealing metabolic memory post-radiochemotherapy", *Nanomedicine: Nanotechnology, Biology and Medicine*, vol. 68, p. 102840, 2025, doi: 10.1016/j.nano.2025.102840. (Q2, IF: 4.6, AIS: 0.776)

4. **R. G. Cozan**, S. Pop, L. M. Crețu, M. Mocan, D. Andraș, D. A. Maniu, I. Mandruțiu, Z. Barabas-Cuzmici, L. Szabó, S. D. Iancu, and N. Leopold, "Surface-enhanced Raman spectroscopy (SERS) metabolite profiling of pleural fluid", *Appl. Phys. Lett.*, vol. 127, no. 25, p. 253703, Dec. 2025, doi: 10.1063/5.0300864 (IF: 3.6, AIS: 0.773).

5. S. D. Iancu, **R. G. Cozan**, A. Ștefancu, M. David, T. Moisoiu, C. Moroz-Dubenco, A. Bajcsi, C. Chira, A. Andreica, L. F. Leopold, D. Eniu, A. Staicu, I. Goidescu, C. Socaciu, D. T. Eniu, L. Diosan, and N. Leopold, "SERS liquid biopsy in breast cancer: What can we learn from SERS on serum and urine?" *Spectrochim. Acta A Mol. Biomol. Spectrosc.*, vol. 273, p. 120992, 2022, doi: 10.1016/j.saa.2022.120992. (Q1, IF: 4.6, AIS: 0.551)

Other publications

1. A. Ștefancu, V. Moisoiu, M. Desmirean, S. D. Iancu, A. B. Țigu, B. Petrushev, A. Jurj, **R. G. Cozan**, L. Budișan, B. Fetica, A. Roman, G. Dobie, C. Turcaș, M. Zdrenghea, P. Teodorescu, S. Pașca, D. Piciu, D. Dima, Z. Bálint, N. Leopold, and C. Tomuleasa, "SERS-based DNA methylation profiling allows the differential diagnosis of malignant lymphadenopathy", *Spectrochim. Acta A Mol. Biomol. Spectrosc.*, vol. 264, p. 120216, 2022, doi: 10.1016/j.saa.2021.120216. (Q1, IF: 4.6, AIS: 0.551)

2. T. Moisoiu, S. D. Iancu, D. Burghelea, M. P. Dragomir, G. Iacob, A. Ștefancu, **R. G. Cozan**, O. Antal, Z. Bálint, V. Muntean, R. I. Badea, E. Licărețe, N. Leopold, and F. I. Elec, "SERS liquid biopsy profiling of serum for the diagnosis of kidney cancer", *Biomedicines*, vol. 10, no. 2, p. 233, 2022, doi: 10.3390/biomedicines10020233. (Q2, IF: 3.9, AIS: 0.89)

3. T. Moisoiu, M. P. Dragomir, S. D. Iancu, S. Schallenberg, G. Birolo, G. Ferrero, D. Burghelea, A. Ștefancu, **R. G. Cozan**, E. Licărețe, A. Allione, G. Matullo, G. Iacob, Z. Bálint, R. I. Badea, A. Naccarati, D. Horst, B. Pardini, N. Leopold, and F. Elec, "Combined miRNA and SERS urine liquid biopsy for the point-of-care diagnosis and molecular stratification of bladder cancer", *Mol. Med.*, vol. 28, 2022, doi: 10.1186/s10020-022-00462-z. (Q1, IF: 6.4, AIS: 1.346)

Conferences

1. **R. G. Cozan**, S. D. Iancu, V. Moisoiu, T. Moisoiu and N. Leopold, "Experimental parameters optimization for reliable urine SERS analysis" in *The 13th International Conference on Advanced Vibrational Spectroscopy* (ICAVS 13), Xiamen, China, Nov. 30-Dec. 05 2025 – poster presentation and flash talk

2. **R. G. Cozan**, S. D. Iancu and N. Leopold, "Refining the SERS Protocol for Urine Analysis in Cancer Diagnostics" in *Women in Photonics*, Jena, Germany, June 1-5, 2025 – oral presentation
3. **R. G. Cozan**, S. D. Iancu and N. Leopold, "SERS liquid biopsy of serum and urine for breast cancer detection" in *The 13th International Conference on Clinical Spectroscopy*, Ioannina, Greece, June 2-4, 2024 – poster presentation
4. **R. G. Cozan**, S. D. Iancu, A. Ștefancu, C. Moroz-Dubenco, A. Bajcsi, C. Chira, L. Diosan, and N. Leopold, "SERS liquid biopsy in breast cancer: What can we learn from SERS on serum and urine?" in *The 17th National Conference of Biophysics* (CNB), Târgu Mureș, Romania, September 23-25, 2022 – poster presentation
5. **R. G. Cozan**, S. D. Iancu, A. Ștefancu, C. Moroz-Dubenco, A. Bajcsi, C. Chira, A. Andreica, L. Diosan, and N. Leopold, "SERS assessment of metabolic variation in serum and urine of breast cancer pacients" in *Metabolomics 2022*, Valencia, Spain, June 19-23, 2022 – poster presentation

Summer schools and other activities

1. EUTOPIA HEALTH Hackathon (September 15-17, 2025, Ljubljana, Slovenia)
2. EUTOPIA Doctoral Summer School 2025 (July 8-22, 2025, Lisbon, Portugal)
3. CLIRSPEC Summer School 2023 (July 17-21, 2023, Windermere, United Kingdom)
4. The International Science and Technology Week (July, 3-7, 2023, Zaragoza, Spain)

INTRODUCTION

Modern medicine is increasingly focused on developing early, accurate, and minimally invasive diagnostic methods. Traditional diagnostic techniques, such as tissue biopsies and imaging, remain widely used but are often invasive and limited in their ability to monitor dynamic molecular changes. Consequently, liquid biopsy approaches based on easily accessible biofluids like blood or urine have gained significant interest in the past few years.

One promising technique for liquid biopsy is surface-enhanced Raman scattering (SERS), which offers high molecular sensitivity and works effectively with biological samples [1-6]. SERS detects molecular vibrational fingerprints through interactions between molecules and plasmonic nanostructures, enabling highly sensitive analysis of biofluids. In label-free SERS, however, the spectra reflect the combined adsorption behavior of multiple biomolecules rather than individual biomarkers. Purine metabolites such as uric acid, hypoxanthine, and xanthine play a major role in these spectra and are associated with diseases including cancer, inflammatory disorders, and cardiovascular conditions.

Despite its potential, clinical implementation of SERS remains challenging due to experimental variability, lack of standardization, and difficulties in interpreting complex biological spectra. Overcoming these limitations requires optimized experimental protocols, advanced data analysis, and validation across multiple clinical settings.

In this context, the present doctoral thesis is situated at the intersection of fundamental SERS methodology and clinical application. By combining controlled experimental design, portable Raman instrumentation, and multivariate data analysis, the primary objective of this thesis is to evaluate and advance label-free SERS as a non-invasive analytical approach for clinical liquid biopsy applications.

1. SURFACE-ENHANCED RAMAN SCATTERING (SERS)

Chapter 1 presents the theoretical foundations of Raman spectroscopy and surface-enhanced Raman scattering (SERS). Raman spectroscopy is a vibrational spectroscopic technique based on the inelastic scattering of light by molecules, providing detailed molecular fingerprints with minimal sample preparation. The Raman effect arises from changes in molecular polarizability during vibration and includes Rayleigh, Stokes, and anti-Stokes scattering processes [7, 8].

However, because only a very small fraction of photons undergo Raman scattering, the sensitivity of conventional Raman spectroscopy is limited [9]. Consequently, enhancement strategies are required to improve detection sensitivity.

In this purpose, SERS spectroscopy was developed as one of the most effective signal amplification techniques, providing enhancement factors up to 10^{14} and enabling single-molecule detection [1-6]. SERS was first observed by Fleischmann *et al.* in 1974 using pyridine adsorbed on rough silver electrodes [10], while the enhancement mechanism was later confirmed independently by Jeanmaire and Van Duyne [11] and Creighton *et al.* [12]. Since then, SERS has become an important topic of research, with its enhancement generally attributed to two complementary mechanisms: electromagnetic enhancement and chemical enhancement [13].

The **electromagnetic enhancement mechanism** originates from localized surface plasmon resonances generated on metallic nanostructures, typically noble metal nanoparticles [14, 15]. When incident light interacts with quasi-free electrons on the metal surface, collective electron oscillations produce highly amplified localized electromagnetic fields near the nanoparticle surface. The intensity of this field depends on nanoparticle size, dielectric properties, and the distance between the molecule and the

metallic surface [16]. Molecules positioned close to the nanostructure experience a dramatic increase in Raman signal intensity due to this amplified electromagnetic field.

In contrast, **the chemical enhancement mechanism** arises from charge-transfer interactions between the adsorbed molecule and the metallic substrate [13, 17]. Adsorption may occur through weak physisorption interactions or stronger chemisorption processes involving orbital hybridization and the formation of metal-molecule complexes [18]. Chemical enhancement is associated with resonant electronic transitions within these complexes, particularly between HOMO and LUMO states, leading to selective amplification of certain vibrational modes [19]. Molecules with high affinity for metal surfaces, such as thiol-containing compounds, readily undergo adsorption and contribute strongly to the SERS effect [20].

Neither electromagnetic nor chemical enhancement alone can fully explain the SERS phenomenon. Therefore, SERS is currently understood as a synergistic interplay between both mechanisms, where chemical enhancement explains the requirement for molecular adsorption and electromagnetic enhancement accounts for the large increase in Raman signal intensity.

2. SERS IN MEDICINE

Chapter 2 presents the biomedical applications of surface-enhanced Raman scattering (SERS), with a particular focus on its use as a label-free liquid biopsy platform. Owing to its high sensitivity, rapid spectral acquisition, low detection limits, compatibility with biological fluids, and minimal sample preparation requirements, SERS has emerged as a promising technique for minimally invasive molecular diagnostics and point-of-care applications [5, 23].

Unlike conventional tissue biopsies, SERS-based liquid biopsy enables the rapid analysis of biofluids without the need for molecular labels or complex sample preparation procedures, providing clinically relevant biochemical information directly from their molecular composition [24] (Figure 2.1.).

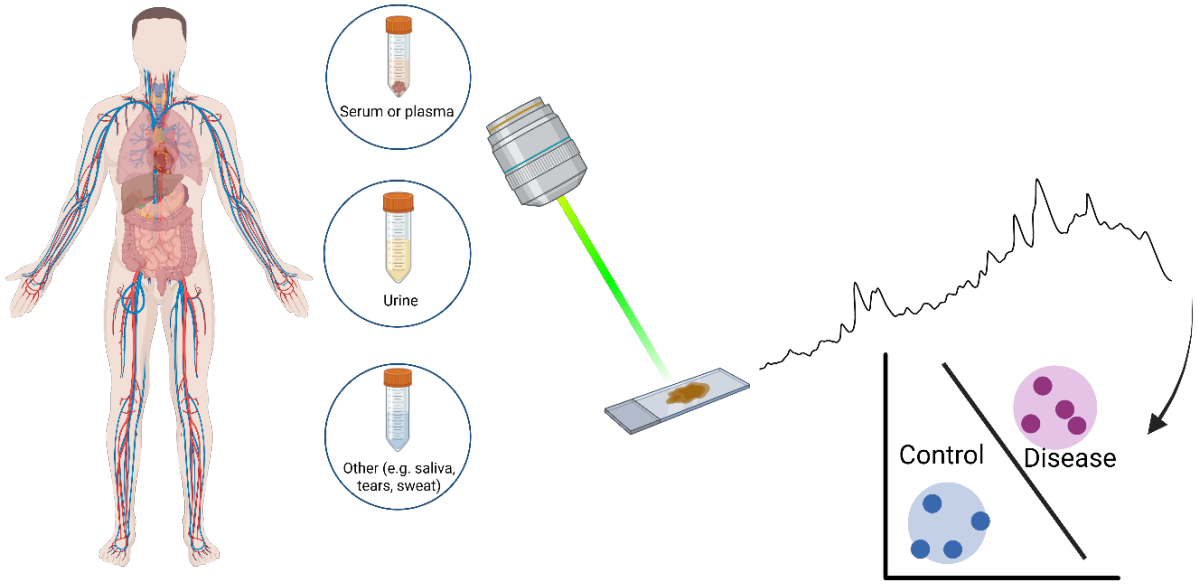

Figure 2.1. Schematic representation of the SERS liquid biopsy workflow, including sample collection, spectral acquisition, and data analysis for sample classification

Furthermore, the diverse applications in oncology [25], infectious diseases [26], metabolic disorders [27], neurological diseases [28], and cardiovascular pathology [29] demonstrates the versatility of SERS for disease detection, classification, and treatment monitoring.

A central aspect of this chapter is the molecular interpretation of label-free SERS spectra of biofluids, based on surface-induced molecular selectivity. Because adsorption processes at the nanoparticle surface preferentially promote the detection of specific molecular species [6, 30], purine metabolites (uric acid, hypoxanthine, and xanthine)

constitute the dominant contributors to the SERS spectra of biofluids (Figure 2.2.). This is attributed to both their high affinity for noble metal surfaces and their relatively high biological concentrations [31-33].

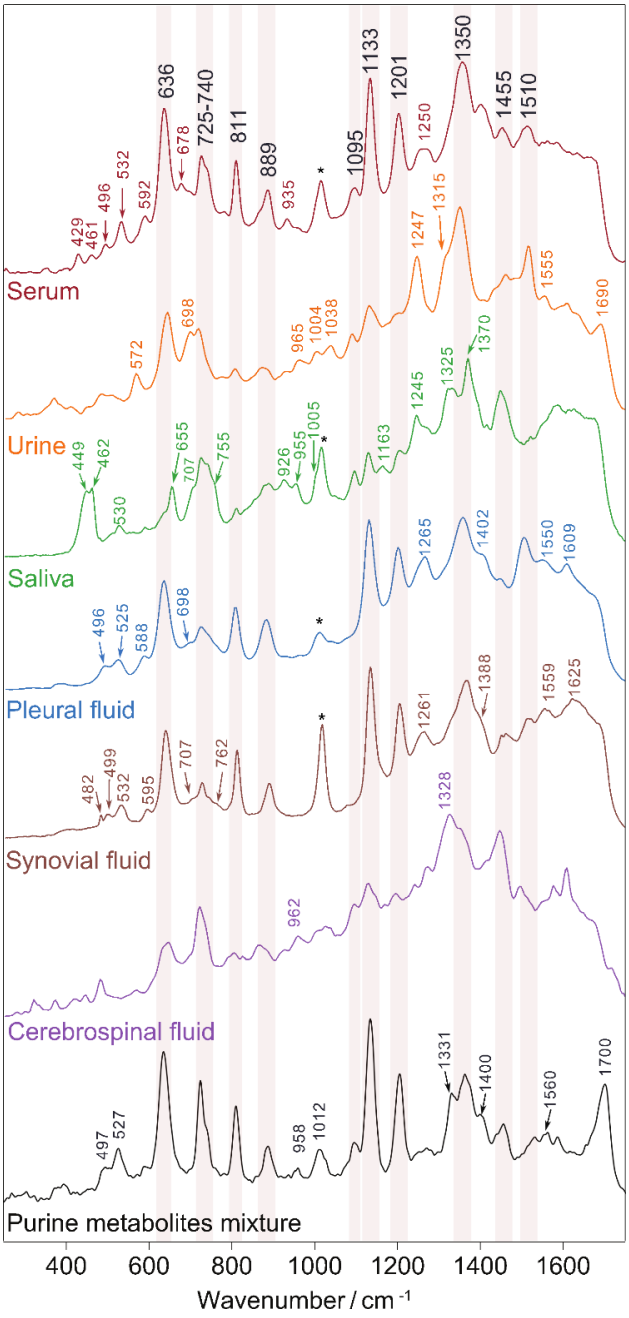

Figure 2.2. SERS spectra of deproteinized blood serum, urine, saliva, pleural, synovial, and cerebrospinal fluid and purine metabolites mixture (10^{-5} M) recorded in a colloidal

AgNPs suspension synthesized via hydroxylamine hydrochloride reduction and recorded using 532 nm laser excitation. Common bands observed across biofluids, characteristic of purine metabolites, are highlighted. * marks the methanol band used for protein removal.

The chapter further emphasizes that biofluid SERS spectra reflect collective adsorption equilibria rather than isolated biomarkers [34, 35]. The recorded spectral profile results from competitive adsorption processes governed by the global biochemical composition of the sample, including metabolite concentration, protein content, pH and surface affinity. Consequently, label-free SERS captures broader metabolic and biochemical alterations associated with disease states, enabling clinically discrimination even in the absence of specific biomarkers.

In addition, Chapter 2 reviews methodological aspects critical for clinical implementation, including sample preprocessing, which improve analyte accessibility and spectral reproducibility [35-41].

Finally, the chapter addresses the major limitations currently hindering the clinical translation of SERS, including substrate variability, lack of standardized experimental protocols, difficulties in spectral interpretation, and challenges related to reproducibility across laboratories and patient cohorts. These considerations establish the conceptual and methodological framework necessary for the experimental investigations presented later in the thesis and underline the importance of optimization and validation for advancing label-free SERS toward routine clinical and point-of-care applications.

3. MATERIALS AND METHODS

This chapter describes the common and general experimental design, sample handling, SERS measurements parameters, and data analysis procedures employed across three independent studies investigating label-free SERS profiling of biofluids: (i) urine-based analysis, (ii) serum-based analysis, and (iii) pleural fluid characterization. Further specific materials and methods characteristic for each study are presented in the corresponding subsections of Chapter 4.

Biofluid samples, including urine, serum, and pleural fluid, were collected from patients with malignant diseases and corresponding control groups following informed consent procedures. To facilitate metabolite detection by SERS, serum and pleural fluid samples underwent centrifugation and methanol-based protein depletion, while urine samples were analyzed in raw form. All preprocessed samples were stored at −80 °C prior to spectral acquisition.

Silver nanoparticles (AgNPs), synthesized through hydroxylamine hydrochloride reduction of silver nitrate according to the Leopold-Lendl method [46], were used as the SERS-active substrate in all experiments.

SERS measurements were performed in clinical environments using portable Raman spectrometers operating with 532 nm laser excitation. For spectral acquisition, biofluid samples were mixed with AgNPs and Ca^{2+} ions prior to deposition onto aluminum-covered microscope slides. The addition of Ca^{2+} ions promoted the adsorption of anionic metabolites onto the nanoparticle surface through mechanisms previously described [47].

Spectra were collected immediately after mixture deposition, with multiple acquisitions averaged to obtain the final spectrum for each sample.

All spectra were processed using a standardized workflow in Quasar-Orange platform [48, 49]. Preprocessing included spectral range selection, baseline correction using a rubber-band algorithm, and vector normalization.

The chapter further details the multivariate statistical: Principal Component Analysis (PCA) was used as an unsupervised dimensionality reduction technique to identify clustering tendencies and extract the dominant variance structure of the spectral datasets, and for classification tasks, the supervised machine learning models Logistic Regression (LR) and Random Forest (RF) were used.

4. RESULTS AND DISCUSSION

4.1 SERS optimization for urine-based early detection of breast cancer

Section 4.1 investigates the application of urine-based surface-enhanced Raman scattering (SERS) as a non-invasive liquid biopsy approach for early breast cancer detection. Although urine SERS analysis represents a promising diagnostic strategy due to its non-invasive collection, minimal preprocessing requirements, and sensitivity to systemic metabolic alterations [50], its clinical implementation is limited by variability in urine composition, particularly pH and dilution, as well as by the incomplete understanding of the molecular contributors to the recorded spectra [35].

This study analyzed urine samples collected from early-stage breast cancer patients (n = 18) and control subjects (n = 10) under controlled pH conditions (pH native, 5, 7, and 9). Sample classification was performed using Principal Component Analysis (PCA) and Logistic Regression (LR).

The study indicates that urinary pH strongly influences molecular adsorption on the silver nanoparticle surface and therefore modulates the resulting SERS spectra. At native

urine pH, spectra were dominated by hypoxanthine bands, whereas alkaline conditions (pH 9) enhanced the contributions of uric acid, hypoxanthine, and creatinine (Figure 4.1.). Xanthine signals decreased under alkaline conditions, likely due to competitive adsorption effects occurring at the nanoparticle interface. Analysis of simulated urine mixtures further confirmed that these spectral variations are governed not only by the intrinsic adsorption properties of individual metabolites, but also by collective adsorption equilibria dependent on pH and molecular competition at the metal surface.

An important finding of this study was the identification of the creatinine band at 1420 cm^{-1} as a suitable internal normalization standard for correcting urine dilution variability. Since creatinine excretion is relatively constant [51], normalization to this band reduced spectral variability associated with hydration status and urine concentration differences, thereby improving the reproducibility and clinical interpretability of the SERS measurements.

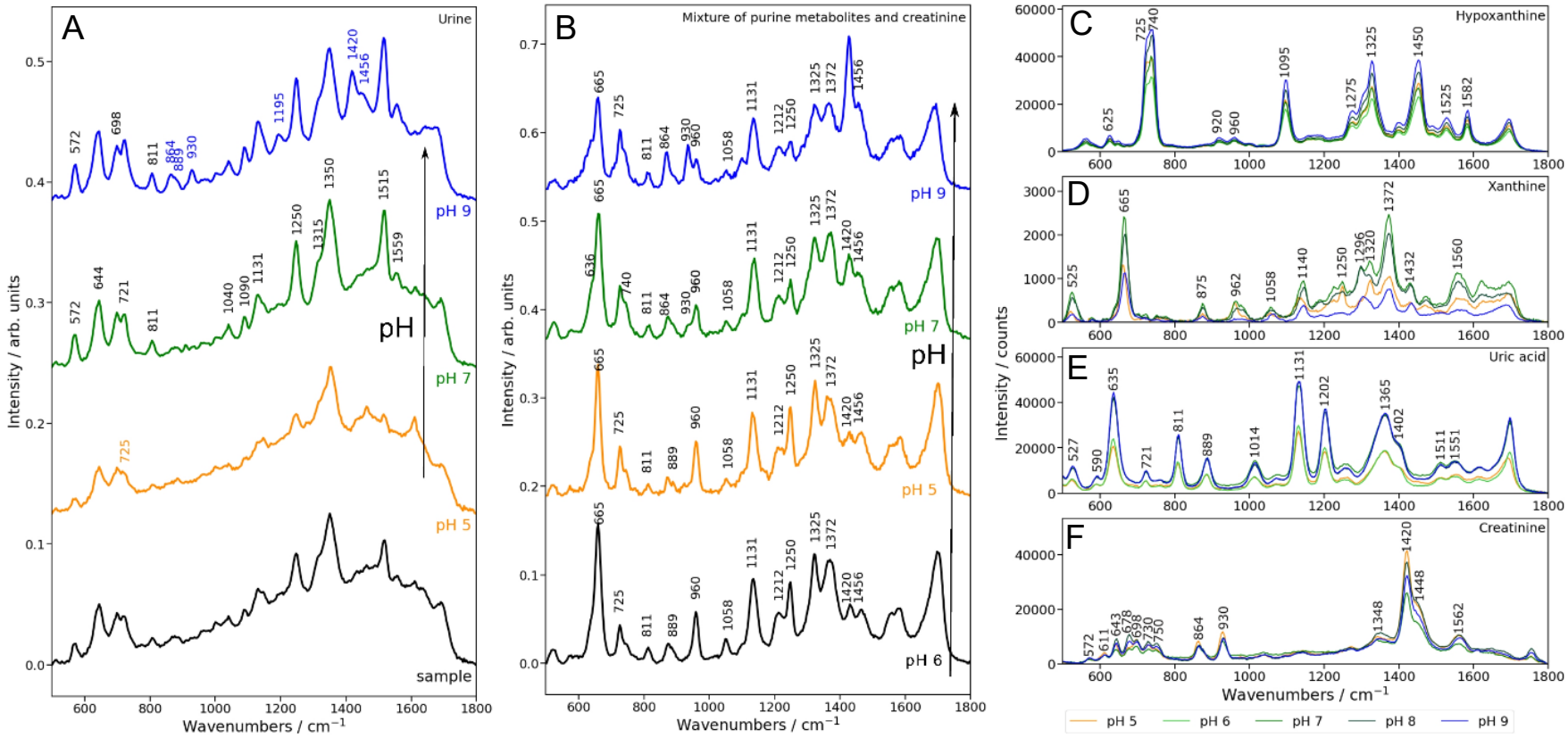

Figure 4.1. Effect of pH on label-free SERS spectral profiles of urine and purine metabolites. (A) Average SERS spectra of urine samples from breast cancer patients at their native pH (black) and after adjustment to pH 5 (orange), pH 7 (green), and pH 9 (blue). (B) SERS spectra of a model mixture containing creatinine (10^{-3} M), uric acid (10^{-4} M), hypoxanthine (10^{-5} M), and xanthine (10^{-5} M), recorded across a pH range from 5 to 9. (C-F) SERS spectra of the individual components measured at different pH values: (C) hypoxanthine, (D) xanthine, (E) uric acid, and (F) creatinine, at pH 5 (orange), pH 6 (light green), pH 7 (green), pH 8 (dark green), and pH 9 (blue) [35]

A visual examination of the SERS spectra highlights clear distinctions between BC and CTRL samples at all investigated pH values, with the richest spectral information being obtained at pH 9. Additionally, the normalization of SERS spectra using the creatinine band at 1420 cm^{-1} revealed marked differences between CTRL and BC groups. In particular, variations were observed in the intensities of bands attributed to hypoxanthine (725 cm^{-1}) and uric acid (889 and 1131 cm^{-1}) (Figure 4.3.A).

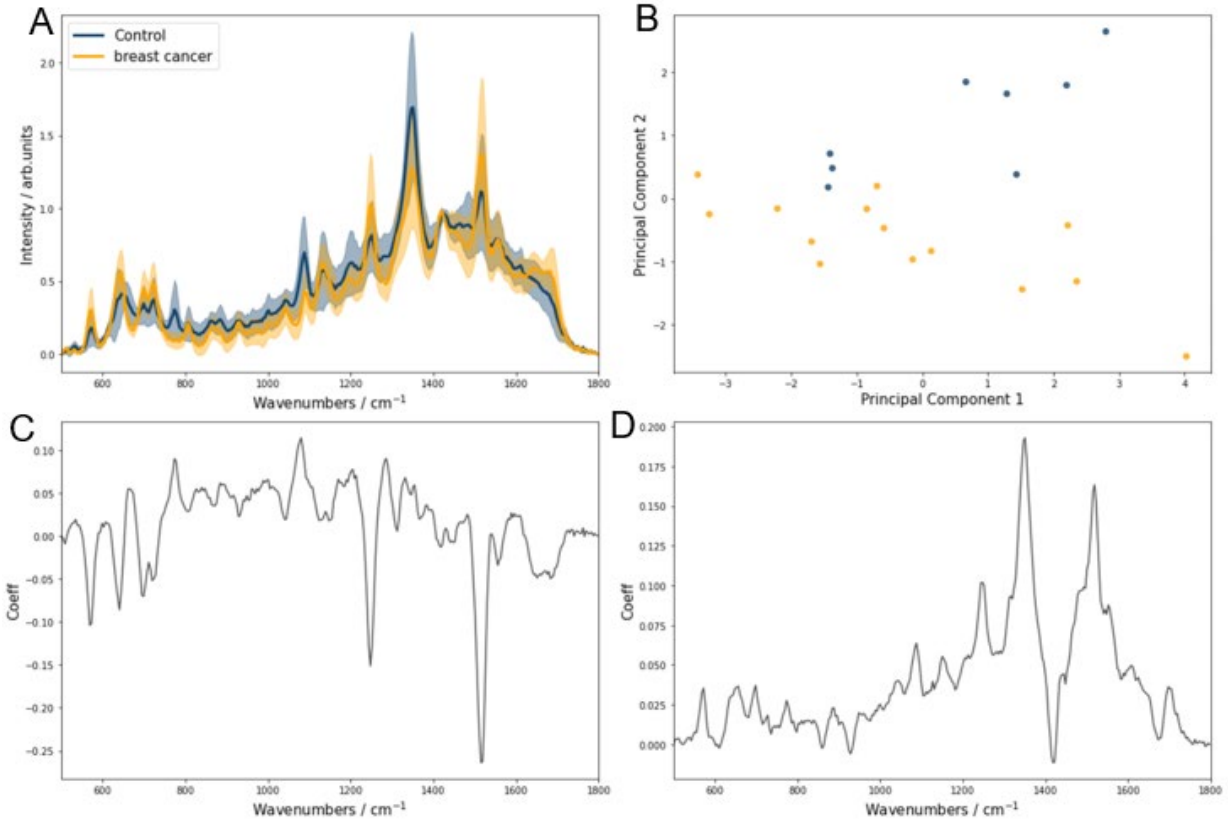

Figure 4.2. (A) Mean SERS spectra of CTRL and BC at pH 9, normalized to the creatinine band at 1420 cm^{-1}, shown with standard deviations. (B) Scatter plot of score values for PC1 and PC2. (C-D) Corresponding loading plots for PC1 (C) and PC2 (D) [35].

The PCA score plot demonstrated unsupervised clustering of the samples, with separation primarily along PC2 (Figure 4.3.B). The corresponding PC2 loading plot indicated a negative correlation between 725, 889 and 1131 cm^{-1} bands with 774, 1080, and 1334 cm^{-1} ones, which could not be assigned to the purine metabolites investigated here and were more prominent in the CTRL group. In contrast, bands related to uric acid and xanthine showed higher intensities in the BC group, underscoring their potential utility as diagnostic markers.

Logistic Regression achieved the highest classification accuracy for urine samples adjusted to pH 9 (89.3%), while creatinine-normalized spectra maintained high classification performance (85.7%) and improved robustness against dilution-related variability.

Overall, this study demonstrates that standardizing urinary pH and applying creatinine-based normalization substantially improve the interpretability, reproducibility, and classification performance of urine SERS analysis. However, the relatively small sample size represents a limitation of the present study, and validation in larger independent cohorts is required.

4.2 Detection and treatment response in colorectal cancer

Section 4.2 explores the applicability of the SERS method for colorectal cancer detection and for evaluating the response of rectal adenocarcinoma (READ) patients to preoperative radiochemotherapy (RCT). Although magnetic resonance imaging (MRI) is routinely used for assessing treatment response prior to surgery, its diagnostic accuracy remains limited and highly dependent on radiological interpretation [52]. Consequently, there is growing interest in non-invasive and objective liquid biopsy approaches capable of monitoring treatment response through systemic metabolic profiling.

This study included serum samples from patients with colon adenocarcinoma (COAD, n = 35), rectal adenocarcinoma treated with RCT (READ, n = 33), and controls with benign pathologies (CTRL, n = 31). Among READ patients, 11 exhibited near-complete tumor regression following RCT (responders, R), while 22 showed residual disease (non-responders, NR), according to the Ryan tumor regression grading system [37]. SERS measurements were performed using portable Raman instrumentation, while processing and interpretation of the spectral data included Principal Component Analysis (PCA) with supervised machine learning models, including Logistic Regression (LR) and Random Forest (RF).

Firstly, the study explored whether SERS spectra acquired from serum could distinguish responders from non-responders following RCT. Mean spectra of responder samples showed higher intensities of bands associated with uric acid and hypoxanthine compared with non-responders, together with a distinct band at 910 cm^{-1} observed only in responders. PCA identified differences between the two groups, primarily through PC5 and PC17.

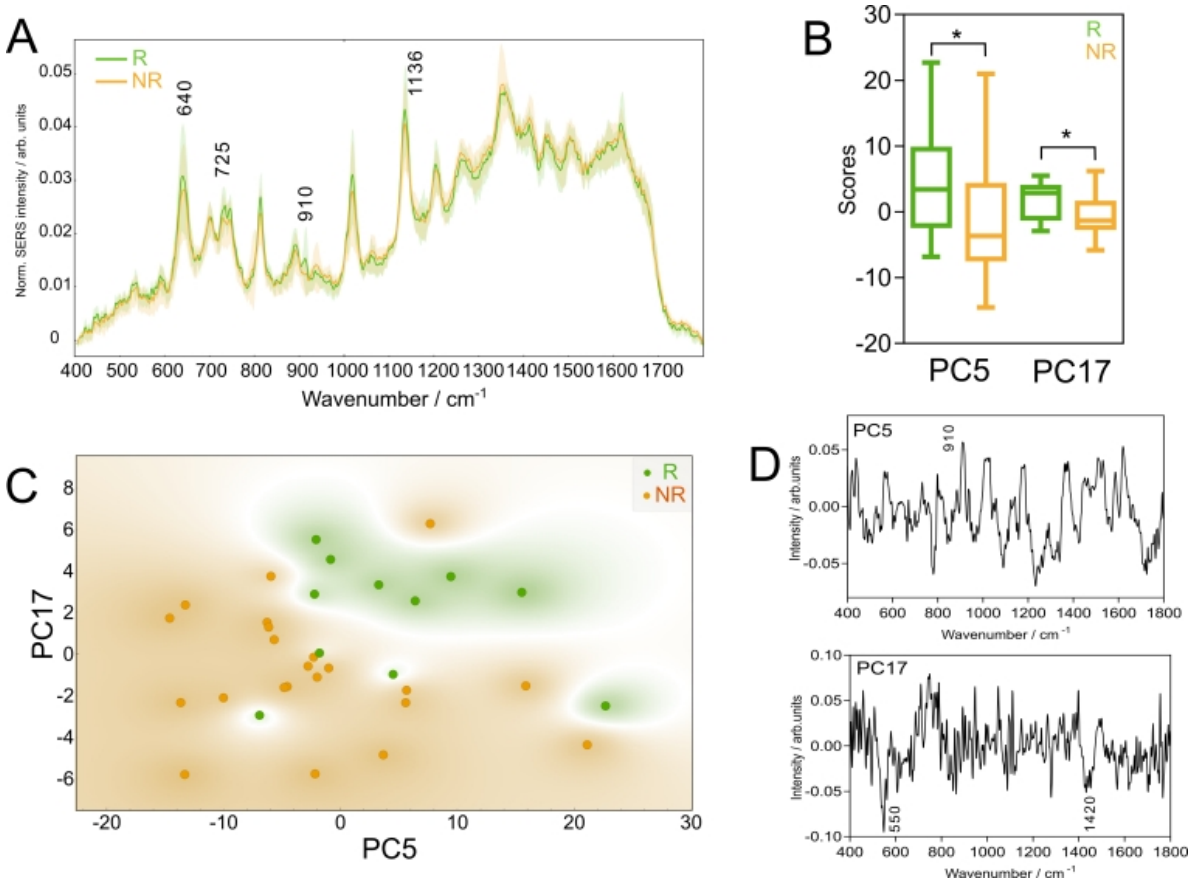

Figure 4.3. (A) Mean serum SERS spectra of patients with READ with almost complete tumor regression (R) and no response (NR) to RCT; (B) Score distributions of PC5 ($p = 0.048$) and PC17 ($p = 0.019$) for R and NR patients; * depicts differences between groups with statistical significance of $p < 0.05$ (C) Sample score plot represented on PC5 and PC17; (D) Loading plots of PC5 and PC17 [53].

A second objective of the study was to determine whether the metabolic signatures of READ patients resembled cancerous or healthy states following treatment. Since COAD and READ share similar histological characteristics, a classification model distinguishing COAD from CTRL samples was developed and subsequently applied independently to the responder and non-responder groups. LR and RF classifiers achieved classification

accuracies of 75% and 74%, respectively, for differentiating COAD from CTRL samples. When applied to the READ cohort, the Random Forest classifier identified 86% of non-responder samples as cancer-related, in agreement with histopathological findings.

Table 4.1. Classification of patients with READ (R and NR to RCT), into COAD and CTRL groups. Confusion matrix of LR and RF classifiers.

		Logistic Regression	**Predicted**	
Actual	**READ**	**Sample**	**COAD**	**CTRL**
		R (n = 11)	8	3
		NR (n = 22)	15	7

		Random Forest	**Predicted**	
Actual	**READ**	**Sample**	**COAD**	**CTRL**
		R (n = 11)	7	4
		NR (n = 22)	19	3

Unexpectedly, most responder samples were also classified as cancer-like despite histopathological evidence of near-complete tumor regression. These findings suggest the persistence of cancer-associated metabolic alterations even after substantial histological tumor regression, supporting the hypothesis of a possible "metabolic memory" effect or residual disease-associated metabolic signature.

Spectral interpretation indicated that the dominant SERS features were primarily associated with purine metabolites such as uric acid, hypoxanthine, and xanthine, whose relative intensities differed between cancer and control groups. In particular, variations in the intensity ratio between the 725 and 740 cm^{-1} bands appeared to contribute to the distinction between cancerous and non-cancerous metabolic profiles.

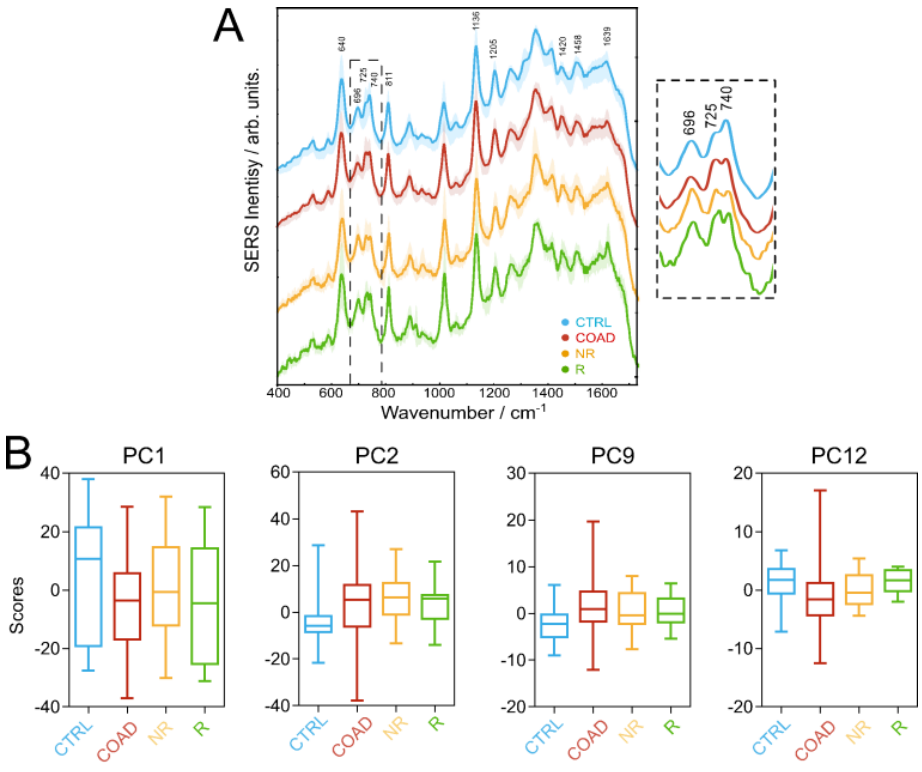

Figure 4.4. (A) Mean SERS spectra of COAD, READ (R and NR) and CTRL samples; (B) The projection of the READ (R and NR), COAD and CTRL spectra on the significant PCs for COAD and CTRL discrimination (PC1, PC2, PC9 and PC12) [53].

Overall, this study demonstrates the potential of serum-based SERS liquid biopsy for both colorectal cancer detection and treatment-response monitoring. The user-independent classification strategy, together with the concordance between SERS-based predictions and histopathological findings, highlights the promise of SERS as a rapid, non-invasive, and clinically adaptable approach for cancer monitoring. Nevertheless, the relatively limited cohort size and the complexity of interpreting biofluid SERS spectra remain important limitations, requiring validation in larger independent cohorts.

4.3 SERS profiling of pleural fluid

Section 4.3 explores the application of surface-enhanced Raman scattering (SERS) for the label-free analysis of pleural fluid, with the aim of developing a rapid and minimally invasive approach for pleural effusion (PE) characterization. Pleural effusions are common complications of pulmonary and systemic diseases, including malignancies, infections, and cardiac disorders, and their diagnosis often relies on specialized laboratory infrastructure. In this context, SERS represents a promising alternative due to its ability to rapidly provide metabolic information from complex biological fluids using portable instrumentation [54-56].

This pilot study investigated SERS profiling of pleural fluid and focused primarily on establishing a practical and reproducible preprocessing workflow. Pleural fluid samples were analyzed in three forms: raw (bulk), centrifuged supernatant, and protein-depleted fractions. Initial measurements of raw and centrifuged samples produced spectra with poor signal quality and limited metabolite information. In contrast, methanol-based protein depletion significantly improved spectral quality and signal-to-noise ratio, demonstrating that protein removal is a critical step for obtaining interpretable pleural fluid SERS spectra.

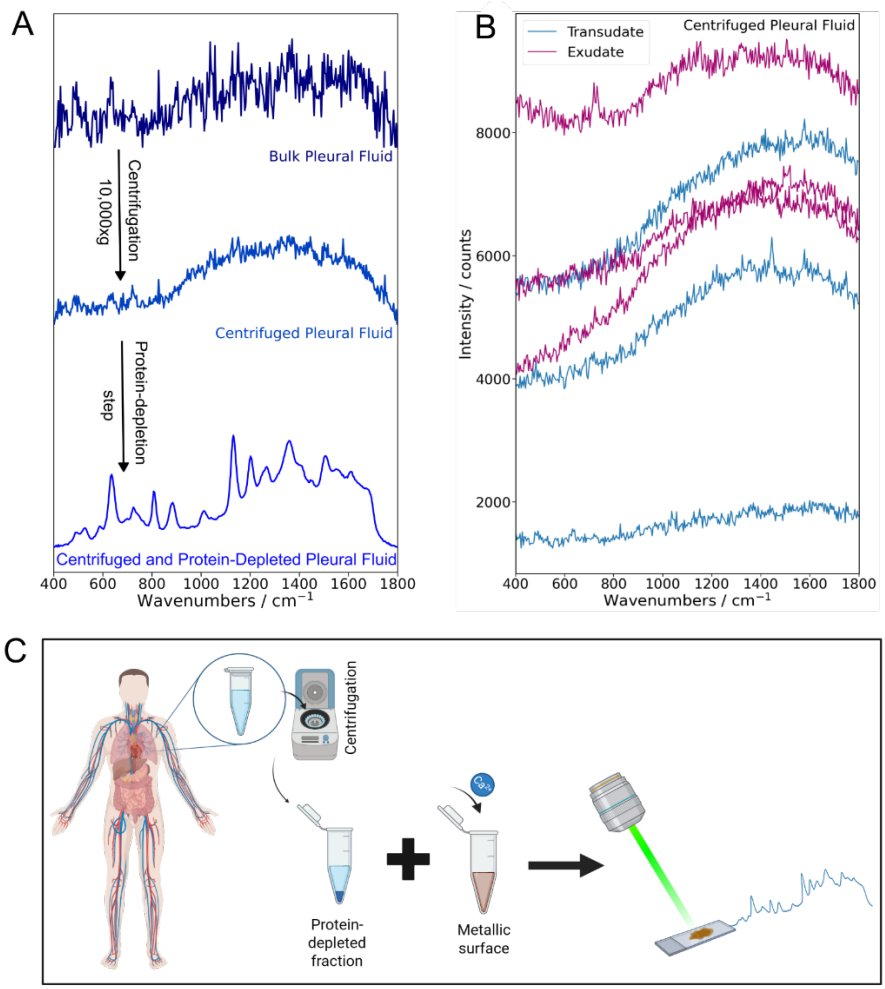

Figure 4.5. (A) The preprocessing steps (bulk sample, centrifuged supernatant, and protein-depleted fluid) alongside the corresponding average SERS spectra. (B) Individual SERS spectra of centrifugated pleural fluid samples, grouped as transudates or exudates. (C) A schematic overview of the experimental workflow for SERS profiling of pleural fluid [57].

A comparative analysis of the SERS spectra of pleural fluid, urine, and serum revealed similar spectral contributions across the three biofluids, with the dominant spectral bands

originating from purine metabolites, particularly uric acid (636, 811, 881, 1130, and 1201 cm^{-1}).

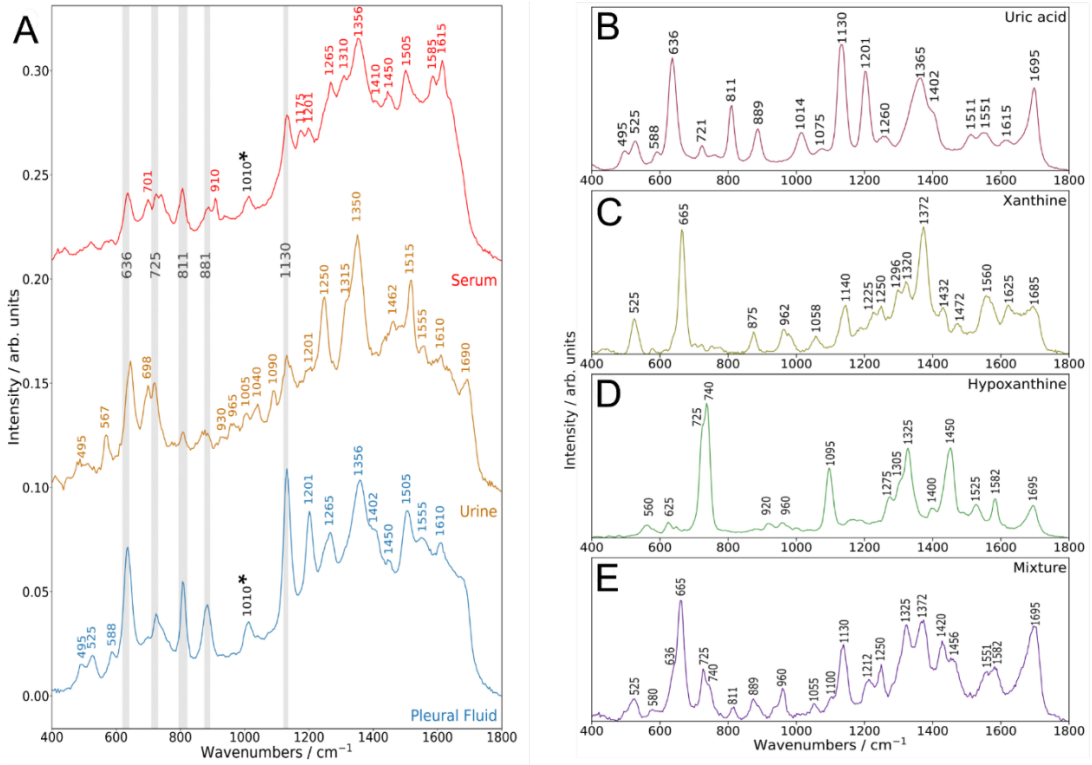

Figure 4.6. (A) Mean SERS spectra of pleural fluid (blue), protein-depleted serum (red) and urine (orange). The Raman band at 1010 cm^{-1} in pleural fluid and serum spectra (marked with *) is attributed to methanol used for sample protein-depletetion. SERS spectra of individual components: (B) uric acid, (C) xanthine and (D) hypoxanthine. (E) SERS spectrum of a mixture containing uric acid, xanthine and hypoxanthine [57].

Subsequently, the study aimed to differentiate between transudative and exudative pleural effusions. Although both groups exhibited broadly similar spectral profiles, differences in relative band intensities and spectral reproducibility were identified.

Transudative samples displayed sharper and more intense uric acid-associated bands together with greater inter-sample variability. In contrast, exudative pleural effusions showed enhanced bands particularly near 725, 740, and 1265 cm^{-1}, and demonstrated improved spectral consistency.

Principal Component Analysis (PCA) further supported the distinction between transudative and exudative samples through unsupervised clustering. Loading plot analysis revealed that the separation was primarily driven by differences between uric acid-dominated spectral regions.

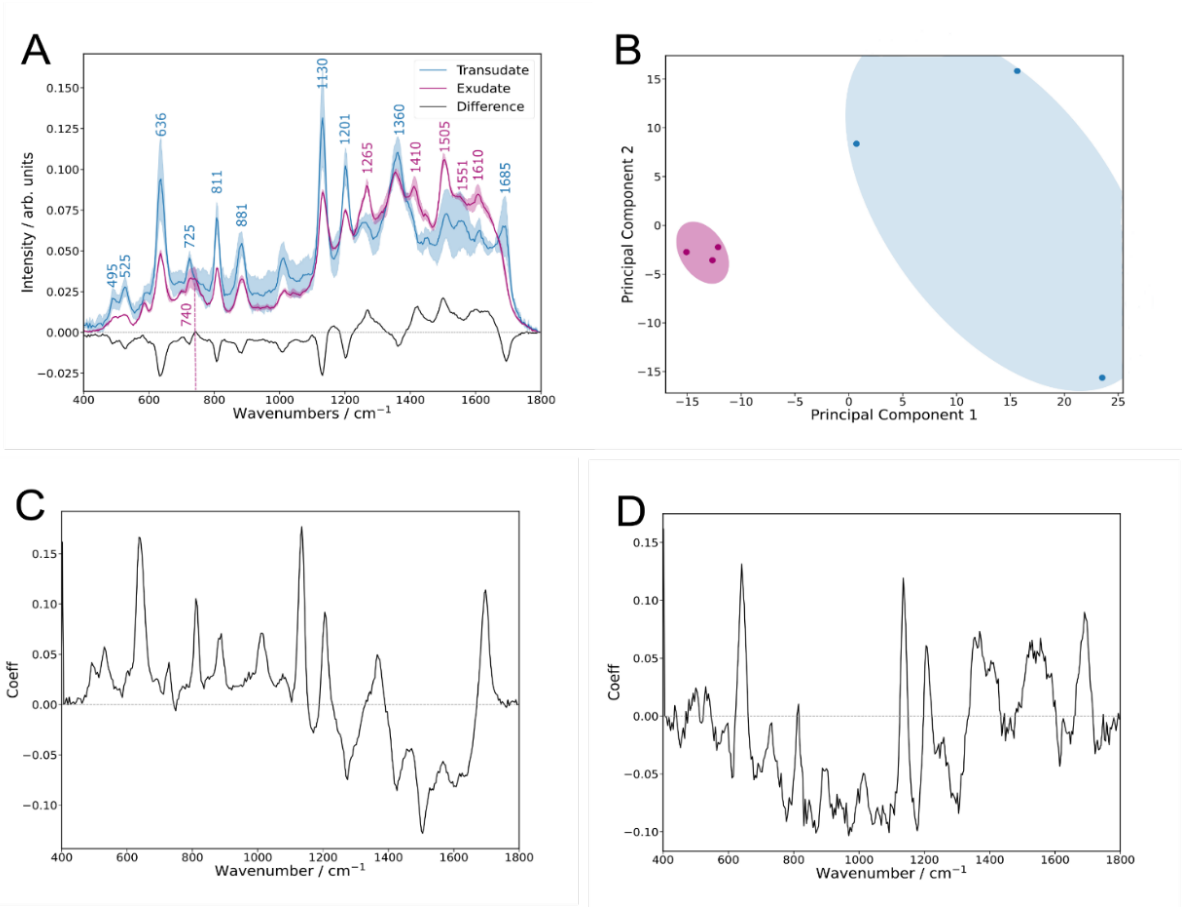

Figure 4.7. (A) Mean SERS spectra and standard deviation of protein-depleted transudate (blue) and exudate (magenta) pleural fluid samples together with their difference

spectrum (black); (B) Scatter plot of PC1 and PC2 score values; Loadings plot of PC1 (C) and PC2 (D) [57].

Overall, this study proposes a workflow for label-free SERS analysis of pleural fluid. The results highlight the potential of SERS as a rapid, cost-effective, and minimally invasive method for pleural fluid characterization, while also emphasizing the importance of standardized preprocessing protocols, particularly protein-depletion. Nevertheless, the relatively small cohort size and exploratory nature of the study require further validation in larger and clinically diverse patient populations.

5. FINAL CONCLUSIONS

Chapter 5 summarizes the main findings of this doctoral thesis and highlights the versatility and clinical potential of SERS spectroscopy as a label-free liquid biopsy method. Through three complementary studies focused on urine, serum, and pleural fluid analysis, this work demonstrates that SERS can detect disease-associated metabolic alterations directly from complex biofluids, supporting its applicability across multiple clinical contexts.

An important achievement across all studies was the successful implementation of portable Raman instrumentation in clinical environments. This demonstrates the feasibility of acquiring SERS spectra outside specialized laboratory settings and supports the potential integration of SERS into point-of-care diagnostic workflows. Combined with automated preprocessing and machine learning analysis, portable SERS systems may reduce operator dependence and improve the accessibility of spectroscopic diagnostics in clinical practice.

Despite these advances, the thesis also highlights several limitations that currently hinder the clinical translation of SERS. Interpretation of label-free SERS spectra remains complex due to overlapping metabolite contributions and the presence of unassigned spectral features. Furthermore, all studies were conducted on relatively small patient cohorts, emphasizing the exploratory nature of the work. Larger multicentric studies, standardized experimental protocols, and further validation will therefore be essential for establishing SERS as a reliable clinical diagnostic technique.

BIBLIOGRAPHY

[1] M. Moskovits, "Surface-enhanced Raman spectroscopy: a brief retrospective", *Journal of Raman Spectroscopy*, vol. 36, no. 6-7, pp. 485-496, 2005/06/01 2005, doi: https://doi.org/10.1002/jrs.1362.

[2] K. Kneipp, Y. Wang, H. Kneipp, L. T. Perelman, I. Itzkan, R. R. Dasari *et al.*, "Single Molecule Detection Using Surface-Enhanced Raman Scattering (SERS)", *Physical Review Letters*, vol. 78, no. 9, pp. 1667-1670, 03/03/ 1997, doi: 10.1103/PhysRevLett.78.1667.

[3] S. Nie and S. R. Emory, "Probing Single Molecules and Single Nanoparticles by Surface-Enhanced Raman Scattering", *Science*, vol. 275, no. 5303, pp. 1102-1106, 1997/02/21 1997, doi: 10.1126/science.275.5303.1102.

[4] P. G. Etchegoin and E. C. Le Ru, "A perspective on single molecule SERS: current status and future challenges", *Physical Chemistry Chemical Physics*, 10.1039/B809196J vol. 10, no. 40, pp. 6079-6089, 2008, doi: 10.1039/B809196J.

[5] J. Langer, D. Jimenez de Aberasturi, J. Aizpurua, R. A. Alvarez-Puebla, B. Auguié, J. J. Baumberg *et al.*, "Present and Future of Surface-Enhanced Raman Scattering", *ACS Nano*, vol. 14, no. 1, pp. 28-117, 2020/01/28 2020, doi: 10.1021/acsnano.9b04224.

[6] A. M. Michaels, M. Nirmal, and L. E. Brus, "Surface Enhanced Raman Spectroscopy of Individual Rhodamine 6G Molecules on Large Ag Nanocrystals", *Journal of the American Chemical Society*, vol. 121, no. 43, pp. 9932-9939, 1999/11/01 1999, doi: 10.1021/ja992128q.

[7] G. Keresztury, "Raman Spectroscopy: Theory", vol. 1, 2006.

[8] N. Leopold, *Surface-Enhanced Raman Spectroscopy. Selected Applications*. Cluj-Napoca: Napoca Star, 2009, p. 155.

[9] R. R. Jones, D. C. Hooper, L. Zhang, D. Wolverson, and V. K. Valev, "Raman Techniques: Fundamentals and Frontiers", (in eng), no. 1931-7573 (Print).

[10] M. Fleischmann, P. J. Hendra, and A. J. McQuillan, "Raman spectra of pyridine adsorbed at a silver electrode", *Chemical Physics Letters*, vol. 26, no. 2, pp. 163-166, 1974/05/15/ 1974, doi: https://doi.org/10.1016/0009-2614(74)85388-1.

[11] D. L. Jeanmaire and R. P. Van Duyne, "Surface raman spectroelectrochemistry: Part I. Heterocyclic, aromatic, and aliphatic amines adsorbed on the anodized silver electrode", *Journal of Electroanalytical Chemistry and Interfacial Electrochemistry*, vol. 84, no. 1, pp. 1-20, 1977/11/10/ 1977, doi: https://doi.org/10.1016/S0022-0728(77)80224-6.

[12] J. A. Creighton, M. G. Albrecht, R. E. Hester, and J. A. D. Matthew, "The dependence of the intensity of Raman bands of pyridine at a silver electrode on the wavelength of excitation", *Chemical Physics Letters*, vol. 55, no. 1, pp. 55-58, 1978/04/01/ 1978, doi: https://doi.org/10.1016/0009-2614(78)85131-8.

[13] J. Yi, E.-M. You, R. Hu, D.-Y. Wu, G.-K. Liu, Z.-L. Yang *et al.*, "Surface-enhanced Raman spectroscopy: a half-century historical perspective", *Chemical Society Reviews*, vol. 54, no. 3, pp. 1453-1551, 2025, doi: 10.1039/d4cs00883a.

[14] G. Haran, "Single-Molecule Raman Spectroscopy: A Probe of Surface Dynamics and Plasmonic Fields", *Accounts of Chemical Research*, vol. 43, no. 8, pp. 1135-1143, 2010/08/17 2010, doi: 10.1021/ar100031v.

[15] E. C. Le Ru, M. Meyer, E. Blackie, and P. G. Etchegoin, "Advanced aspects of electromagnetic SERS enhancement factors at a hot spot", *Journal of Raman Spectroscopy*, vol. 39, no. 9, pp. 1127-1134, 2008/09/01 2008, doi: https://doi.org/10.1002/jrs.1945.

[16] J. A. Koningstein, *Introduction to the Theory of the Raman Effect*. Dordrecht-Holland: D. Reidel Plublishing Company, 1971.

[17] A. T. a. H. Zayak, Y. S. and Choo, H. and Bokor, J. and Cabrini, S. and Schuck, P. J. and Neaton, J. B., "Chemical Raman Enhancement of Organic Adsorbates on Metal Surfaces", *Physical Review Letters*, vol. 106, 2011, doi: 10.1103/physrevlett.106.083003.

[18] A. Dąbrowski, "Adsorption — from theory to practice", *Advances in Colloid and Interface Science*, vol. 93, no. 1, pp. 135-224, 2001/10/08/ 2001, doi: https://doi.org/10.1016/S0001-8686(00)00082-8.

[19] J. a. F. Ziroff, F. and Schöll, A. and Puschnig, P. and Reinert, F., "Hybridization of Organic Molecular Orbitals with Substrate States at Interfaces: PTCDA on Silver", *Physical Review Letters*, vol. 104, 2010, doi: 10.1103/physrevlett.104.233004.

[20] C. Vericat, M. Vela, G. Corthey, E. Pensa, E. Cortés, M. H. Fonticelli *et al.*, "Self-Assembled Monolayers of Thiolates on Metals: A Review Article on Sulfur-Metal Chemistry and Surface Structures", *RSC Advances*, vol. 4, p. 27730, 11/18 2014, doi: 10.1039/c4ra04659e.

[21] H. Xu, E. J. Bjerneld, M. Käll, and L. Börjesson, "Spectroscopy of Single Hemoglobin Molecules by Surface Enhanced Raman Scattering", *Physical Review Letters*, vol. 83, no. 21, pp. 4357-4360, 11/22/ 1999, doi: 10.1103/PhysRevLett.83.4357.

[22] V. Brabec and K. Niki, "Raman scattering from nucleic acids adsorbed at a silver electrode", *Biophysical Chemistry*, vol. 23, no. 1, pp. 63-70, 1985/11/01/ 1985, doi: https://doi.org/10.1016/0301-4622(85)80064-8.

[23] D. Cialla-May, X. S. Zheng, K. Weber, and J. Popp, "Recent progress in surface-enhanced Raman spectroscopy for biological and biomedical applications: from cells to clinics", *Chemical Society Reviews*, 10.1039/C7CS00172J vol. 46, no. 13, pp. 3945-3961, 2017, doi: 10.1039/C7CS00172J.

[24] K. Kneipp, H. Kneipp, I. Itzkan, R. R. Dasari, and M. S. Feld, "Surface-enhanced Raman scattering: A new tool for biomedical spectroscopy", *Current Science*, vol. 77, no. 7, pp. 915-924, 1999. [Online]. Available: http://www.jstor.org/stable/24103661.

[25] L. Ma, H. Guo, Y. Zhao, Z. Liu, C. Wang, J. Bu *et al.*, "Liquid biopsy in cancer: current status, challenges and future prospects", *Signal Transduction and Targeted Therapy,* vol. 9, no. 1, p. 336, 2024/12/02 2024, doi: 10.1038/s41392-024-02021-w.

[26] P. Eiamchai, C. Juntagran, P. Somboonsaksri, U. Waiwijit, J. Eisiri, J. Samarnjit *et al.*, "Determination of latent tuberculosis infection from plasma samples via label-free SERS sensors and machine learning", *Biosensors and Bioelectronics,* vol. 250, p. 116063, 2024/04/15/ 2024, doi: https://doi.org/10.1016/j.bios.2024.116063.

[27] S. Li, Y. Zheng, Y. Yang, H. Yang, C. Han, P. Du *et al.*, "Diagnosis and classification of intestinal diseases with urine by surface-enhanced Raman spectroscopy", *Spectrochimica Acta Part A: Molecular and Biomolecular Spectroscopy,* vol. 312, p. 124081, 2024/05/05/ 2024, doi: https://doi.org/10.1016/j.saa.2024.124081.

[28] H. Jiang, Y. Zhang, L. Zhang, L. Liu, H. Wang, Y. Wang *et al.*, "Comprehensive Serum Analysis via an AI-Assisted Magnetically Driven SERS Platform for the Diagnosis and Etiological Differentiation of Childhood Epilepsy", *ACS Applied Materials & Interfaces,* vol. 17, no. 8, pp. 11731-11741, 2025/02/26 2025, doi: 10.1021/acsami.4c19603.

[29] A. C. Espinosa-Garavito, E. N. Quiroz, N. J. Galán-Freyle, G. Aroca-Martinez, S. P. Hernández-Rivera, J. Villa-Medina *et al.*, "Surface-enhanced Raman Spectroscopy in urinalysis of hypertension patients with kidney disease", *Scientific Reports,* vol. 14, no. 1, p. 3035, 2024/02/06 2024, doi: 10.1038/s41598-024-53679-9.

[30] S. E. J. Bell and N. M. S. Sirimuthu, "Surface-Enhanced Raman Spectroscopy (SERS) for Sub-Micromolar Detection of DNA/RNA Mononucleotides", *Journal of the American Chemical Society,* vol. 128, no. 49, pp. 15580-15581, 2006/12/01 2006, doi: 10.1021/ja066263w.

[31] M. Pagliai, S. Caporali, M. Muniz-Miranda, G. Pratesi, and V. Schettino, "SERS, XPS, and DFT Study of Adenine Adsorption on Silver and Gold Surfaces", *The Journal of Physical Chemistry Letters,* vol. 3, no. 2, pp. 242-245, 2012/01/19 2012, doi: 10.1021/jz201526v.

[32] Y. Dong, J. Ma, J. Bian, Q. Zou, T. Jiang, C. Zhao *et al.*, "Reliable detection of uric acid in urine by SERS technique on three-dimension carbon framework decorated with Ag nanoparticles", *Journal of Molecular Liquids,* vol. 423, p. 127020, 2025/04/01/ 2025, doi: https://doi.org/10.1016/j.molliq.2025.127020.

[33] C. Westley, Y. Xu, B. Thilaganathan, A. J. Carnell, N. J. Turner, and R. Goodacre, "Absolute Quantification of Uric Acid in Human Urine Using Surface Enhanced Raman Scattering with the Standard Addition Method", *Analytical Chemistry,* vol. 89, no. 4, pp. 2472-2477, 2017/02/21 2017, doi: 10.1021/acs.analchem.6b04588.

[34] A. Bonifacio, S. Dalla Marta, R. Spizzo, S. Cervo, A. Steffan, A. Colombatti *et al.*, "Surface-enhanced Raman spectroscopy of blood plasma and serum using Ag and Au nanoparticles: a systematic study", *Analytical and bioanalytical chemistry,* vol. 406, no. 9-10, pp. 2355-65, Apr 2014, doi: 10.1007/s00216-014-7622-1.

[35] D. Andraș, R. G. Cozan, D. E. Muresan, V. Moisoiu, G. Crișan, V. Binţinţan *et al.*, "Advancing Breast Cancer Diagnosis: Optimization of Raman Spectroscopy for Urine-Based Early Detection", Article vol. 13, no. 2, 2025, Art no. 505, doi: 10.3390/biomedicines13020505.

[36] T. T. Kouri, W. Hofmann, R. Falbo, M. Oyaert, S. Schubert, J. B. Gertsen *et al.*, "The EFLM European Urinalysis Guideline 2023", *Clinical Chemistry and Laboratory Medicine (CCLM),* vol. 62, no. 9, pp. 1653-1786, 2024, doi: 10.1515/cclm-2024-0070.

[37] G. Del Mistro, S. Cervo, E. Mansutti, R. Spizzo, A. Colombatti, P. Belmonte *et al.*, "Surface-enhanced Raman spectroscopy of urine for prostate cancer detection: a preliminary study", (in eng), *Analytical and bioanalytical chemistry,* vol. 407, no. 12, pp. 3271-5, May 2015, doi: 10.1007/s00216-015-8610-9.

[38] X. Cui, T. Liu, X. Xu, Z. Zhao, Y. Tian, Y. Zhao *et al.*, "Label-free detection of multiple genitourinary cancers from urine by surface-enhanced Raman spectroscopy", *Spectrochimica Acta Part A: Molecular and Biomolecular Spectroscopy,* vol. 240, p. 118543, 2020/10/15/ 2020, doi: https://doi.org/10.1016/j.saa.2020.118543.

[39] D. Hu, X. Xu, Z. Zhao, C. Li, Y. Tian, Q. Liu *et al.*, "Detecting urine metabolites of bladder cancer by surface-enhanced Raman spectroscopy", *Spectrochimica Acta Part A: Molecular and Biomolecular Spectroscopy,* vol. 247, p. 119108, 2021/02/15/ 2021, doi: https://doi.org/10.1016/j.saa.2020.119108.

[40] P. Bernini, I. Bertini, C. Luchinat, P. Nincheri, S. Staderini, and P. Turano, "Standard operating procedures for pre-analytical handling of blood and urine for metabolomic studies and biobanks", *Journal of Biomolecular NMR,* vol. 49, no. 3, pp. 231-243, 2011/04/01 2011, doi: 10.1007/s10858-011-9489-1.

[41] T. Moisoiu, M. P. Dragomir, S. D. Iancu, S. Schallenberg, G. Birolo, G. Ferrero *et al.*, "Combined miRNA and SERS urine liquid biopsy for the point-of-care diagnosis and molecular stratification of bladder cancer", *Molecular Medicine,* vol. 28, no. 1, p. 39, 2022/04/01 2022, doi: 10.1186/s10020-022-00462-z.

[42] Y. Lin, Q. Zhang, H. Chen, S. Liu, K. Peng, X. Wang *et al.*, "Multi-cancer early detection based on serum surface-enhanced Raman spectroscopy with deep learning: a large-scale case–control study", *BMC Medicine,* vol. 23, no. 1, p. 97, 2025/02/21 2025, doi: 10.1186/s12916-025-03887-5.

[43] M. S. Al Ja'farawy, V. T. N. Linh, J.-Y. Yang, C. Mun, S. Lee, S.-G. Park *et al.*, "Whole urine-based multiple cancer diagnosis and metabolite profiling using 3D evolutionary gold nanoarchitecture combined with machine learning-assisted SERS", *Sensors and Actuators B: Chemical,* vol. 412, p. 135828, 2024/08/01/ 2024, doi: https://doi.org/10.1016/j.snb.2024.135828.

[44] N. Gao, Q. Wang, J. Tang, S. Yao, H. Li, X. Yue *et al.*, "Non-invasive SERS serum detection technology combined with multivariate statistical algorithm for simultaneous screening of cervical cancer and breast cancer", *Analytical and Bioanalytical Chemistry,* vol. 413, no. 19, pp. 4775-4784, 2021/08/01 2021, doi: 10.1007/s00216-021-03431-3.

[45] Y. Mi, X. Li, X. Zeng, Y. Cai, X. Sun, Y. Yan *et al.*, "Diagnosis of neuropsychiatric systemic lupus erythematosus by label-free serum microsphere-coupled SERS fingerprints with machine learning", *Biosensors and Bioelectronics,* vol. 260, p. 116414, 2024/09/15/ 2024, doi: https://doi.org/10.1016/j.bios.2024.116414.

[46] N. Leopold and B. Lendl, "A New Method for Fast Preparation of Highly Surface-Enhanced Raman Scattering (SERS) Active Silver Colloids at Room Temperature by Reduction of Silver Nitrate with Hydroxylamine Hydrochloride", *The Journal of Physical Chemistry B,* vol. 107, no. 24, pp. 5723-5727, 2003/06/01 2003, doi: 10.1021/jp027460u.

[47] G. Ion, Chiriac A., M., Ciceo-Lucacel R., A., Moisoiu V., Stefancu A., Iancu S., D. and Leopold N., "Role of Ca2+ in SERS: surface Ag+ formation and anion adsorption - a mechanistic approach", *Romanian Reports in Physics,* vol. In Press: https://rrp.nipne.ro/IP/AP849.pdf, 2026. [Online]. Available: https://rrp.nipne.ro/IP/AP849.pdf.

[48] M. R. Toplak, Stuart; borondics; Levandoski, João E.; Solheim, Johanne; oroue; Blazhko, Vlad; larazupan; Noah; Ajda; achimkohler; Godec, Primož; 1rafaelmayer; Tisor, Austin; Sammut, Letizia; rafael; Rosendahl, Scott M.; Kumar, Rahul, "Quasars/orange-spectroscopy: Release 0.5.8 (Version 0.5.8). Zenodo", 2021, doi: http://doi.org/10.5281/zenodo.4617978.

[49] M. Toplak, S. T. Read, C. Sandt, and F. Borondics, "Quasar: Easy Machine Learning for Biospectroscopy", vol. 10, no. 9, p. 2300, 2021. [Online]. Available: https://www.mdpi.com/2073-4409/10/9/2300.

[50] S. D. Iancu, R. G. Cozan, A. Stefancu, M. David, T. Moisoiu, C. Moroz-Dubenco *et al.*, "SERS liquid biopsy in breast cancer. What can we learn from SERS on serum and urine?", *Spectrochimica Acta Part A: Molecular and Biomolecular Spectroscopy,* vol. 273, p. 120992, 2022/05/15/ 2022, doi: https://doi.org/10.1016/j.saa.2022.120992.

[51] L. Selistre, V. de Souza, C. Nicola, L. Juillard, S. Lemoine, and L. Derain-Dubourg, "Average creatinine–urea clearance: revival of an old analytical technique?", *Clinical Kidney Journal,* vol. 16, no. 8, pp. 1298-1306, 2023, doi: 10.1093/ckj/sfad050.

[52] M.-Z. Wei, Z.-H. Zhao, and J.-Y. Wang, "The diagnostic accuracy of magnetic resonance imaging in restaging of rectal cancer after preoperative chemoradiotherapy: a meta-analysis and systematic review", *Journal of Computer Assisted Tomography,* vol. 44, no. 1, pp. 102-110, 2020.

[53] D. Andras, S. D. Iancu, R. G. Cozan, M. Zetes, G. Crisan, C. F. Buldus *et al.*, "SERS liquid biopsy in colorectal cancer detection and treatment response: Revealing metabolic memory post-radiochemotherapy", *Nanomedicine: Nanotechnology, Biology and Medicine,* vol. 68, p. 102840, 2025/08/01/ 2025, doi: https://doi.org/10.1016/j.nano.2025.102840.

[54] J. M. Porcel and R. W. Light, "Diagnostic approach to pleural effusion in adults", *American Family Physician,* vol. 73, pp. 1211-1220, 2006, doi: 10.1378/chest.105.5.1338.

[55] E. E. McGrath and P. B. Anderson, "Diagnosis of Pleural Effusion: A Systematic Approach", *American Journal of Critical Care,* vol. 20, no. 2, pp. 119-128, 2011, doi: 10.4037/ajcc2011685.

[56] Z. Chen, Y. Wang, and M. Fang, "Analysis of tumor markers in pleural effusion and serum to verify the correlations between serum tumor markers and tumor size, TNM stage of lung adenocarcinoma", *Cancer Medicine,* vol. 9, no. 4, pp. 1392-1399, 2020, doi: 10.1002/cam4.2809.

[57] R. G. Cozan, S. Pop, L. M. Creţu, M. Mocan, D. Andraş, D. A. Maniu *et al.*, "Surface-enhanced Raman spectroscopy (SERS) metabolite profiling of pleural fluid", *Applied Physics Letters,* vol. 127, no. 25, p. 253703, 2025, doi: 10.1063/5.0300864.